Assignment 2 TFY4235: Vibrations of Fractal Drums

Haakon Monclair

ABSTRACT

This study investigates the vibrational properties of a quadratic Koch fractal drum, focusing on the eigenfrequencies, eigenmodes, and the density of states. By numerically solving the Helmholtz equation using finite difference methods, we computed the eigenmodes and eigenfrequencies of the fractal drum and analyzed the scaling behavior of the density of states in relation to the Weyl-Berry conjecture. The eigenmodes exhibited strong localization, a result of the fractal geometry creating regions of high curvature and narrow "throats" that impede wave propagation. According to the Weyl-Berry conjecture, the deviation $\Delta N(\omega) = \frac{A}{4\pi}\omega^2 - N(\omega)$ is expected to scale as ω^d, where d is the fractal dimension of the boundary. Our numerical results for the quadratic Koch fractal (with $d = 3/2$) show good agreement with this prediction, providing support for the conjecture. Additionally, the eigenmodes of the clamped thin plate problem showed even stronger localization due to the Neumann boundary condition. The results highlight the unique behavior of waves in fractal geometries and suggest potential applications in acoustics and materials science. This study provides a computational framework for exploring the vibrational properties of fractal drums and contributes to the ongoing investigation of the Weyl-Berry conjecture.

I. INTRODUCTION

The study of vibrating membranes, such as drums, has long been a topic of interest in both physics and mathematics. A fundamental question in this field was posed by Mark Kac in 1966: "Can one hear the shape of a drum?"[1]. This question explores whether the eigenfrequencies of a drum (its "sound") can uniquely determine its shape. While Kac's work focused on smooth boundaries, the introduction of fractal boundaries—geometrical shapes with non-integer dimensions—adds a new layer of complexity and intrigue. Fractal drums, characterized by their intricate, self-similar boundaries, exhibit unique vibrational properties that differ significantly from those of traditional drums. Understanding these properties not only deepens our knowledge of wave dynamics in complex geometries but also has potential applications in materials science, acoustics, and even quantum mechanics.

The vibrational modes of a drum are governed by the Helmholtz equation, which arises from the wave equation under the assumption of harmonic time dependence. For a drum with a smooth boundary, the eigenfrequencies and eigenmodes are well-studied, and their relationship to the drum's geometry is described by the Weyl conjecture[2]. However, when the boundary becomes fractal, the situation changes dramatically. Fractal boundaries introduce localized vibrations and strong damping effects, as demonstrated experimentally by Sapoval et al.[3]. These localized modes are a direct consequence of the fractal geometry, which creates regions of high curvature and narrow "throats" that impede wave propagation.

The Weyl-Berry conjecture extends the Weyl conjecture to fractal boundaries, proposing that the deviation $\Delta N(\omega) = \frac{A}{4\pi}\omega^2 - N(\omega)$ scales as ω^d, where d is the fractal dimension of the boundary[4,5]. This conjecture remains an open problem in mathematical physics, and numerical studies of fractal drums provide valuable insights into its validity.

In this project, we investigate the vibrational properties of a quadratic Koch fractal drum, a specific type of fractal boundary with a known fractal dimension $d = 3/2$. This is done by creating the Koch Square Fractal[6] and solving the Helmholtz equation on its domain. The main objectives are finding the eigenfrequencies and eigenmodes of the fractal drum, as well as studying the density of states with respect to the Weyl-Berry conjecture[4].

This report is organized as follows: Section 2 outlines the theoretical background and models employed in the study. Section 3 presents the results, followed by an analysis and discussion. Lastly, Section 4 provides a summary of the main conclusions of this work.

II. MODELS AND METHODS

A. Theoretical background and equations

1. *The Helmholtz Equation*

The vibrations of a drum are governed by the wave equation. In our case we are working with a 2D surface, so the wave equation reads as follows:

$$\nabla^2 u(\mathbf{x},t) = \frac{1}{v^2}\frac{\partial^2}{\partial t^2}u(\mathbf{x},t), \tag{1}$$

where ∇^2 is called the Laplacian. To study the eigenmodes and eigenfrequencies of our system we separate the variables and apply Dirichlet boundary conditions[7] and we end up with the Helmholtz equation

$$-\nabla^2 U(\mathbf{x}) = \frac{\omega^2}{v^2}U(\mathbf{x}), \quad \text{with} \quad U(\mathbf{x}) = 0 \quad \text{on} \quad \partial\Omega. \tag{2}$$

Here $U(\mathbf{x})$ is the displacement of the wave, ω is the frequency and $\partial\Omega$ is the boundary of the quadratic Koch curve. This equation takes the form of an eigenvalue problem.

To solve this we have to discretize the Helmholtz equation. This is done by approximating the Laplacian operator in equation (2) with a finite difference scheme. We used both

a 5-point and a 9-point[8] stencil to approximate. The 5-point stencil is shown in equation (3):

$$-\frac{1}{\delta^2}\left[U_{m+1,n}+U_{m-1,n}+U_{m,n+1}+U_{m,n-1}-4U_{mn}\right] = \frac{\omega^2}{v^2}U_{mn}, \tag{3}$$

here m and n denote x and y coordinates. In the solution we also multiply both sides by the length L^2, so that we actually calculate the dimensionless eigenvalues $\lambda = \frac{\omega^2}{v^2}L^2$.

2. *The Weyl-Berry conjecture*

The Weyl conjecture (1911) provides a relationship between the geometry of a domain and the distribution of its eigenfrequencies. For a two-dimensional domain Ω with a smooth boundary, the integrated density of states (IDOS) $N(\omega)$ (the number of eigenfrequencies less than ω) asymptotically behaves as:

$$N(\omega) = \frac{A}{4\pi}\omega^2 - \frac{L}{4\pi}\omega + ..., \tag{4}$$

where A is the area of the surface and L is the perimeter. For domains with fractal boundaries, the Weyl conjecture does not hold, as the perimeter is not well-defined. Instead, Berry (1979) proposed a generalization known as the Weyl-Berry conjecture[4,5]. For a fractal drum with a boundary of fractal dimension d, the IDOS is conjectured to scale as:

$$N(\omega) = \frac{A}{4\pi}\omega^2 - C_d M\omega^d + ..., \tag{5}$$

where C_d and M are constants. From this it follows that the deviation between the experimental results, and the Weyl-Berry conjecture looks like

$$\Delta N(\omega) = \frac{A}{4\pi}\omega^2 - N(\omega), \tag{6}$$

and this quantity scales with ω^d. This conjecture remains unproven in general, and numerical studies of fractal drums provide valuable insights into its validity.

3. *Clamped thin plate*

Lastly in this study we investigate the vibrational modes of the *clamped thin plate*. This is described by the following equations:

$$\nabla^4 W(\mathbf{x},\omega) = \lambda W(\mathbf{x},\omega) \quad \text{in} \quad \Omega, \tag{7}$$

$$W(\mathbf{x},\omega) = 0 \quad \text{on} \quad \partial\Omega, \tag{8}$$

$$\frac{\partial W(\mathbf{x},\omega)}{\partial n} = 0 \quad \text{on} \quad \partial\Omega. \tag{9}$$

Here we have both Dirichlet boundary conditions (zero on boundary) and Neumann boundary conditions[7], which means that the normal derivative on the boundary should also be zero. The operator ∇^4 is called the biharmonic operator and is approximated using a 13-point stencil[9].

B. Fractal creation

The quadratic Koch fractal is constructed from a single straight line, which is divided into eight equal segments. Each of these segments is then further divided into eight equal parts, and this process continues iteratively, creating an increasingly intricate pattern. The assembly of such a fractal is shown in Figure 1.

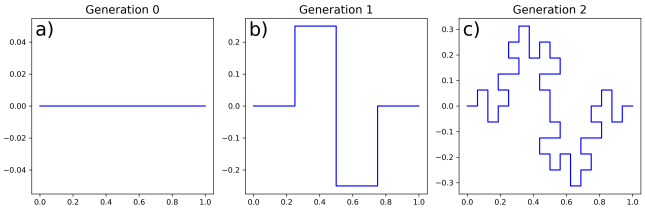

FIG. 1. Creation of a Koch square fractal of a line from generation 0 to generation 2.

This was coded in Python using a recursive method. I first created a function that does the step going from generation 0 to generation 1 (from a to b in Figure 1). This was then applied recursively until reaching the base case where the sought after level of the fractal was reached. This recursive function was applied to a square of length L = 1, and the resulting function was saved as a $N \times 2$ NumPy[10] array, where each row element corresponds to a coordinate (x, y). The resulting Koch square is shown in Figure 2.

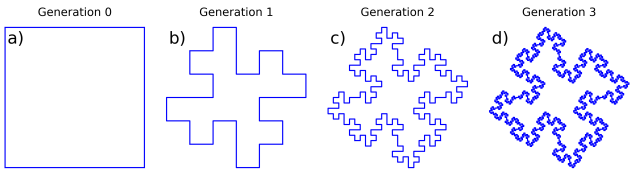

FIG. 2. Final creation of a Koch square fractal, from generation 0 to generation 3.

C. Lattice and matrix generation

I then created a lattice for each refinement level ℓ with points at each corner of the Koch fractal. The length between each of the lattice points is determined by the level and it was found to follow the equation

$$\delta = \frac{L}{4^\ell}. \tag{10}$$

The lattice was created using NumPy function `meshgrid`[10]. A visualization of the lattice is shown in Figure 3.

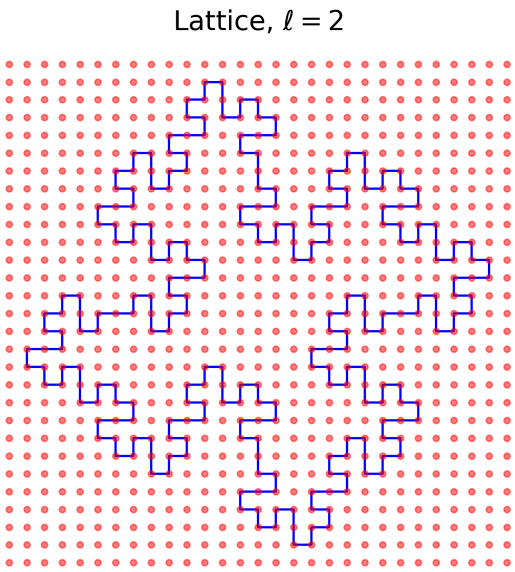

FIG. 3. Visualization of the lattice with points at each corner of the Koch square for level $\ell = 2$.

This lattice was then used to classify each of the lattice points and create a classification matrix. Each of the points outside the Koch curve where given the value 0, points on the boundary were given value -1, and points inside were given values from 1 and upwards. Finding out which points are on the inside of a closed curve is the tricky part, however it is a well known problem with many known algorithms. The method I used is a widely known ray-casting algorithm, with the even-odd rule. This works in that from each point we cast a ray (a straight line) and count how many times it intercepts the boundary. If the number of intercepts is odd, the point is inside the curve, while if its even, the point is outside. Practically this was done by using the Matplotlib library[11] to create a path of the Koch square and then use the `contains_points` function which uses a ray-casting approach.

The result of this is a classification matrix that we use to create our Laplacian matrices to use in our eigenproblem from equation (3).

D. Creating the Laplacian Matrix

The Laplacian matrices were created by the following approach:

1. Take the classification matrix and create a list with all the indices of the points inside the Koch square.
2. Iterate through the list with inside indices. For each index, we:
   - Assign the center element of the matrix corresponding to that point with a coefficient, centerCoeff, which represents the diagonal term of the Laplacian. This coefficient is based on the spatial properties of the lattice, including the parameter L (size scale) and δ (grid spacing) according to the stencil used.
   - For each point, we check its neighbors. If a neighbor is also within the lattice (i.e., it lies inside the Koch square), the corresponding elements of the matrix are updated with a coefficient based on what approximation of the Laplacian we are using. This coefficient corresponds to the interaction between neighboring lattice points in the Laplacian matrix.
3. Transform the matrix into a sparse matrix.

The resulting matrix is a very sparse matrix with elements only around the diagonal. Thus step number 3 is necessary to create a sparse Scipy[12] matrix that is much more manageable than a normal Numpy array.

E. Solving the system

After creating the Laplacian matrices from section II D we can solve the eigenproblem. Since we store the final matrix as a sparse matrix we use the ARPACK[13] library as our eigensolver. It is slower than the highly efficient LAPACK[14] library used in Numpy, but that would require way too much memory for our large matrices (for level 4 the Laplacian matrix has shape 57435×57345), thus the ARPACK library found in the Scipy library works good for this system.

After finding the eigenvectors we need to map them into a new lattice so that they can be visualized. This is done simply by creating a new lattice and at each index corresponding to an inside point we assign the corresponding value from our eigenvector.

F. Investigating the Weyl-Berry conjecture

Firstly I calculated the first 1000 eigenvalues for both level 3 and level 4. I then calculated the IDOS (Integrated Density Of States), and $\Delta N(\omega)$ from equation (6). From the Weyl-Berry conjecture[4] we know that this quantity is supposed to scale with ω^d thus I plot ΔN vs ω in a log-log plot and fit a line with linear regression. The slope of this line represents the value of d.

G. Clamped thin plate problem

The matrix for the biharmonic operator, ∇^4, was created in a similar way as the Laplacians in section II D, with a 13-

point stencil and the addition of the boundary condition from equation (9). This new boundary condition was handled with the use of ghost points. For the 13-point stencil we have to check points that are 2 unit lengths away from our central point. This means that occasionally we can reach a point that lies outside our Koch square. To enforce the Neumann boundary condition, which requires the normal derivative to vanish at the boundary, we approximate it by assigning the value of the ghost point (outside the domain) to be equal to the value at the nearest point inside the boundary, effectively mirroring the value across the boundary. This results in a symmetric difference across the boundary. For example, consider the finite difference approximation for the derivative in the x-direction:

$$\frac{\partial u}{\partial x} \approx \frac{u(x+h,y)-u(x-h,y)}{2h} = 0, \tag{11}$$

when $u(x+h,y) = u(x-h,y)$. By setting the ghost point equal to the interior point, the difference vanishes, satisfying the Neumann condition $\frac{\partial u}{\partial n} = 0$ at the boundary.

III. RESULTS

A. Eigenvalues and eigenvectors of the Helmholtz equation

Table I presents the first ten eigenvalues computed using both the 5-point and 9-point finite difference approximations. The eigenvalues are expressed in the form $\frac{\omega}{v}L$, and results from both level 3 and 4 are included. As observed, the differences between the levels are minimal, indicating good convergence.

Index	5-point stencil		9-point stencil	
	Level 3	Level 4	Level 3	Level 4
1	9.4268	9.4299	9.4268	9.4205
2	14.1420	14.1469	14.1420	14.1242
3	14.1420	14.1469	14.1420	14.1242
4	14.4138	14.4199	14.4138	14.3960
5	14.4889	14.4969	14.4889	14.4737
6	15.0622	15.0824	15.0622	15.0664
7	15.0622	15.0824	15.0622	15.0664
8	17.6321	17.6559	17.6321	17.6345
9	18.8849	18.9114	18.8849	18.8857
10	19.4167	19.4563	19.4167	19.4302

TABLE I. First 10 eigenvalues $\frac{\omega}{v}L$ for the 5-point and 9-point stencil methods at refinement levels 3 and 4.

The eigenmodes corresponding to the first eight eigenvalues at refinement level 4, obtained using the 5-point method, are presented in Figure 4. We clearly see that the vibrations become localized to specific regions, in contrast to a normal drum square or circular drum. Although the eigenmodes in Figure 4 are computed using the 5-point method, those obtained with the 9-point method appear very similar — as expected, given the close agreement in eigenvalues shown in Table I.

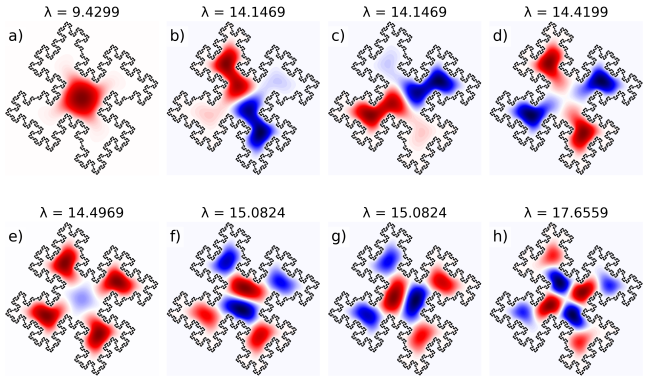

FIG. 4. Eigenmodes corresponding to the first eight eigenvalues at refinement level 4, calculated using the 5-point stencil method. The modes are visualized for the corresponding eigenvalues to illustrate their spatial distributions.

B. Weyl-Berry conjecture analysis

The plots in Figure 5 show the log-log plots of ΔN vs ω. From Figure 5a) we see that the data points undergo a sharp decline towards the end. This is due to a higher degree of degeneracy among the larger eigenvalues at fractal level 3, which results in a poor linear fit and an inaccurate estimate of the d-value. However we see from Figure 5b) that for level 4 there is a very good fit, and the value d is very close to the theoretical value 1.5. This hints to the Weyl-Berry conjecture being correct even though it still isn't rigorously proved. Increasing the level further would likely increase the accuracy as its dependent on the boundary properties, however if we increase ℓ we would quickly meet problems such as floating-point precision and huge memory requirements as the matrices grow exponentially with higher level.

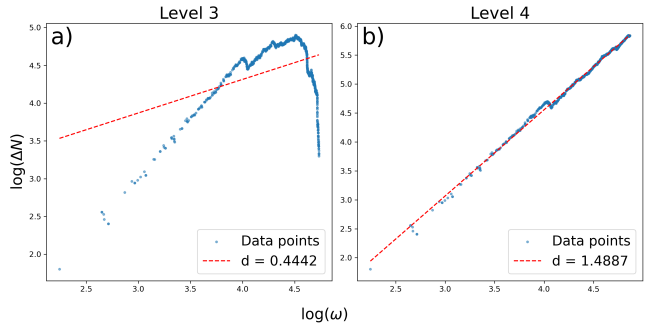

FIG. 5. Log-log plots of ΔN versus ω, illustrating the relationship between the change in the number of states and the frequency parameter. The red lines represent linear regression fits. Panel 5a) shows the results for level 3, while 5b) presents the results for level 4.

C. Clamped thin plate

Figure 6 shows the eigenmodes and corresponding eigenvalues obtained from the clamped thin plate problem. Compared to the standard fractal drum modes in Figure 4, we observe even stronger localization of vibrations. This increased localization can be attributed to the Neumann boundary condition, which effectively reflects waves back into the domain, reducing energy leakage.

The fractal Koch boundary, with its intricate geometry of narrow necks and inward-pointing corners, already acts to confine and scatter wave motion. The addition of Neumann conditions reinforces this effect by enhancing wave interference within these confined regions. As a result, vibrational energy becomes more spatially concentrated, giving rise to highly localized modes within the fractal structure.

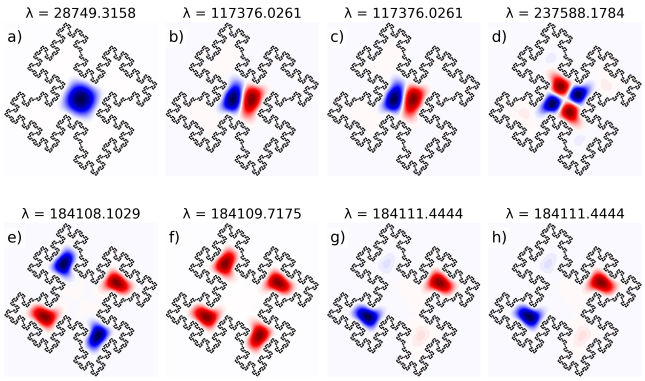

FIG. 6. Eigenmodes of the clamped thin plate corresponding to the first eight eigenvalues at refinement level 4.

IV. CONCLUSIONS

In this study, we investigated the vibrational properties of a quadratic Koch fractal drum, focusing on the eigenfrequencies, eigenmodes, and the density of states. By solving the Helmholtz equation using finite difference methods, we found that the eigenmodes exhibit strong localization due to the fractal geometry, which consists of regions with high curvature and narrow "throats" that impede wave propagation. The eigenvalues computed using both the 5-point and 9-point stencils showed good agreement, with minimal differences between refinement levels 3 and 4, indicating robust convergence of the numerical methods.

The integrated density of states $N(\omega)$ was analyzed, and the deviation $\Delta N(\omega) = \frac{A}{4\pi}\omega^2 - N(\omega)$ was examined in relation to the Weyl-Berry conjecture. According to the conjecture, $\Delta N(\omega)$ is expected to scale as ω^d, where d is the fractal dimension of the boundary. For the quadratic Koch fractal, the fractal dimension is $d = 3/2$. At refinement level 4, the scaling of $\Delta N(\omega)$ closely matched the theoretical prediction, with $d \approx 1.5$, providing numerical evidence in support of the Weyl-Berry conjecture. However, the conjecture remains unproven in general, and further work is needed to explore its applicability to other fractal geometries.

The eigenmodes of the clamped thin plate problem exhibited even stronger localization compared to the standard fractal drum, a result of the Neumann boundary condition reflecting waves back into the domain and enhancing wave interference within the fractal structure. This increased localization highlights the unique behavior of waves in fractal geometries and suggests potential applications in acoustics and materials science.

While the finite difference methods used in this study are effective for moderate refinement levels, they become computationally expensive for higher levels due to the exponential growth of the Laplacian matrices. Future work could extend this study to higher refinement levels or explore alternative numerical methods to address the challenges faced when increasing refinement. Additionally, the methods developed here could be applied to other fractal geometries or extended to three-dimensional systems.

V. REFERENCES

[1] M. Kac, "Can one hear the shape of a drum?" American Mathematical Monthly **73**, 1–23 (1966).

[2] H. Weyl, "Das asymptotische verteilungsgesetz der eigenwerte linearer partieller differentialgleichungen," Mathematische Annalen **71**, 441–479 (1911).

[3] B. Sapoval, T. Gobron, and A. Margolina, "Vibrations of fractal drums," Physical Review Letters **67**, 2974–2977 (1991).

[4] M. V. Berry, "Distribution of modes in fractal resonators," in *Structural Stability in Physics* (Springer, 1979).

[5] C. Hua and B. D. Sleeman, "Fractal drums and the n-dimensional modified weyl-berry conjecture," Communications in Mathematical Physics **168**, 581–607 (1995).

[6] Q. Li, C. Du, and Y. Jiang, "Koch curve and fractal dimension determination," Chinese Journal of Engineering **22**, 354–357 (2000), in Chinese, with English abstract.

[7] L. C. Evans, *Partial Differential Equations*, 2nd ed. (American Mathematical Society, 2010) p. 120.

[8] Y. Oono and S. Puri, "Computationally efficient modeling of ordering of quenched phases," Physical Review Letters **58**, 836–839 (1987).

[9] A. B. M. Hamed, M. H. A. Hashim, M. A. Ahmed, M. B. S. K., and R. K. S., "Finite difference approximation method of biharmonic equation in human face recognition," International Journal of Advances in Computer Science and Technology **2**, 111–114 (2013).

[10] T. E. Oliphant *et al.*, "Numpy v1.21.0 documentation," (2021), accessed: 2023-03-17.

[11] J. D. Hunter *et al.*, "Matplotlib documentation," (2021), accessed: 2023-03-17.

[12] E. Jones *et al.*, "Scipy: Open source scientific tools for python," (2021), accessed: 2023-03-17.

[13] R. Lehoucq, D. C. Sorensen, and C. Yang, *ARPACK Users Guide: Solution of Large-Scale Eigenvalue Problems with Implicitly Restarted Arnoldi Method* (SIAM, Philadelphia, 1998).

[14] E. Anderson, Z. Bai, C. Bischof, S. Blackford, J. D. J. Dongarra, J. D. Croz, A. Greenbaum, S. Hammarling, A. McKenney, and D. Sorensen, *LAPACK Users' Guide, 3rd ed.* (SIAM, Philadelphia, Pennsylvania, 1999).